Coalescence of holes in two-dimensional free-standing smectic films

P. V. Dolganov, N. S. Shuravin, and V. K. Dolganov
Institute of Solid State Physics, Russian Academy of Sciences, Chernogolovka, Moscow Region 142432, Russia

(Received 4 February 2020; accepted 31 March 2020; published 4 May 2020)

We investigate in free-standing smectic films coalescence of holes (circular regions with thickness smaller than the surrounding film). This process can be considered as a two-dimensional analog of coalescence of bubbles in a three-dimensional fluid. A high speed video camera was used to study the evolution of domains at different stages of coalescence. Special attention was given to investigations of the dependence of the size of the bridge between two holes at the initial stage of coalescence, which was considered in numerous theoretical works and bears information on the coalescence mechanism. It is established that the scaling law is applicable for the description of the transformation of bridges for holes of different radius R. We found that in the regime corresponding to the experimental situation the length of the bridge H increases with the scaling law $H/R = (t/\tau_R)^{1/2}$. The characteristic time τ_R determined from the scaling law is larger than the theoretical time, which can be connected with dissipation of energy both in the film and inside the holes.

DOI: 10.1103/PhysRevE.101.052701

I. INTRODUCTION

Coalescence of droplets and bubbles is a common phenomenon widespread in nature and relevant for numerous technical applications. In spite of its apparent simplicity the description of coalescence is a nontrivial fundamentally important task. During coalescence a substantial transformation of the particle geometry takes place, and different dynamical regimes of the liquid flow can be realized. This is the reason why the exact analytical solution of the problem about the form of domains at different stages of coalescence was obtained only for two cylinders in the viscous coalescence regime [1–4]. Difficulties of numerical calculations are in particular due to a large number of material parameters, complex geometry of domains, and dynamics of coalescence. Scaling laws which proved to be useful in various fields of physics are now widely used for the description of coalescence.

The most characteristic changes take place at the initial stage of coalescence in the region of the bridge between two droplets or bubbles. A large number of theoretical and experimental studies are devoted to investigation of coalescence of droplets and the early time evolution of the bridge radius r_m [5–15]. The temporal transformation of the domain depends on the magnitude of so-called Ohnesorge number $\mathrm{Oh} = \eta/(\rho R\gamma)^{1/2}$, where η and γ are the viscosity of the liquid and the surface tension of the domain boundary, ρ is the liquid density, and R is the initial radius of the droplet [13,14]. It was predicted that there exist viscous, when $\mathrm{Oh} \gg 1$, and inertial, when $\mathrm{Oh} \ll 1$, regimes of coalescence. In some cases a so-called "inertially limited viscous" regime is observed [10–12]. The driving force is the Laplace pressure near the end of the bridge $p \sim \gamma R/{r_m}^2$. In the inertial regime this pressure competes with the inertial stress $\rho(dr_m/dt)^2$. The temporal dependence of the bridge radius $r_m \sim (\gamma R/\rho)^{1/4}(t)^{1/2}$ [6,13]. Scaling r_m by R and t by inertial-capillary time $\tau_i = (\rho R^3/\gamma)^{1/2}$ [6,13] allows us to rewrite the equation in a simple dimensionless form, $r_m/R \sim (t/\tau_i)^{1/2}$. The subscript i denotes the inertial regime. Experimental investigations of droplets confirmed the growth of the bridge as the square root of time [12,14].

In the viscous regime the situation is more complicated [7–9,13]. For the early stage the simplest dependence which follows from scaling $r_m(t)/R = F(t/\tau_v)$ is the linear variation of $r_m(t)/R$ with time $r_m(t)/R \sim t/\tau_v$. The subscript v represents the viscous regime. A similar dependence [$r_m(t)$ is proportional to time] was observed in a number of experimental studies at the early stage of droplet coalescence [7,8]. Linear dependence was also found in the "inertial limited viscous" regime [10–12]. Eggers *et al.* [5] predicted the logarithmic correction to the linear dependence, that is, the length of the bridge radius $r_m(t)$ has to increase as $r_m(t)/R \sim (t/\tau_v)\ln(t/\tau_v)$. Such behavior was observed in coalescence of nematic domains on a water substrate [9]. So, dependence of r_m on time in the viscous regime is complicated. Two-dimensional (2D) coalescence of islands [16–19] and oil droplets [20] was investigated in free-standing smectic films (FSSFs) [21]. FSSFs are formed by flat smectic layers parallel to the surfaces which border with air. Islands are regions with thickness larger than the film. FSSFs provide a unique possibility to study coalescence in a quasi-two-dimensional system. The analytical Hopper solution [1–4] was used for analysis of island coalescence [16–18]. It was shown [18,20] that experimental data for island and droplet coalescence can be described by Hopper's solution.

Theory and experiment show that complex behavior can be realized for coalescence of bubbles in an outer fluid [22–24]. Paulsen *et al.* [22] considered the situation when the fluid medium exists both outside and inside the bubble, but the viscosity of outer and inner fluids η_{out} and η_{in} differ. For $\eta_{\mathrm{out}} \gg \eta_{\mathrm{in}}$ a crossover can be observed between the regimes in which the main role is played by the inner and outer fluid flow [22]. Recent simulations of bubble coalescence [24] show that the length of the bridge can grow as the square root of time both in the inertial and viscous regime

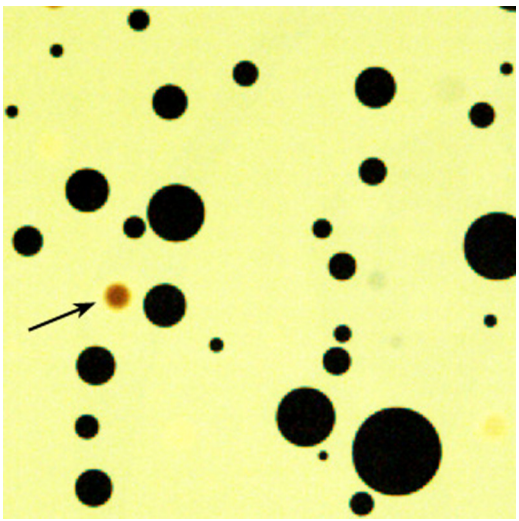

FIG. 1. Free-standing smectic film with holes (dark circular regions) whose thickness is smaller than the thickness of the film. The arrow indicates a smectic island with thickness greater than the thickness of the film. The horizontal size of the image is 450 μm.

but with different dependencies of the characteristic times τ_R on material parameters.

The simplest 2D analogs of 3D bubbles are holes in FSSFs. Holes are the regions of FSSFs whose thickness is smaller than the thickness of the outer smectic film. In this paper we present the experimental study of coalescence of holes in thin 2D free-standing smectic films and analyze in detail the behavior of coalescence using scaling theory. We show that the length of the bridge $2H(t)$ can be described in the framework of the scaling law $H(t)/R \sim (t/\tau_R)^{1/2}$ when $\eta_{\rm out} \sim \eta_{\rm in}$.

II. EXPERIMENTAL DETAILS

Experiments were conducted on smectic *A* (Sm*A*) liquid crystal 4-n-octylcyanobiphenyl (8CB, Kingston Chemicals). This material forms the Sm*A* phase in the temperature interval 21–33 °C. The long molecular axes in the Sm*A* phase are perpendicular to the plane of smectic layers. The procedure employed to prepare FSSFs and holes in FSSFs was described earlier [25–28]. We used two methods to obtain the holes in the film. In the first method the film was prepared on a rectangular frame with two moveable sides. After preparing the film, its area was rapidly increased by shifting the moveable sides of the frame; as a result, holes appeared in the film. In the second method, holes were obtained by blowing gently on the film with an air jet. The material of the film is sheared and regions of different thickness (islands and holes) can appear in the film. When the air jet is stopped, created holes and islands remain in the film. The structure of holes does not depend on the method of preparation. Relatively small holes are obtained in our experiment (typical radii were from about 50 to 140 μm). As a rule, when films are prepared they have regions with different numbers of smectic layers and holes of different size and thickness. Figure 1 shows a typical smectic film with holes of different sizes (dark circular regions). For further experiments we selected films with a uniform thickness. The coalescence of holes with the same thickness and approximately the same size was investigated. The size and depth of the holes was determined before as well as in the process of coalescence. We provide data for pairs of holes with difference in sizes from about 5% to about 20%. Since the size of coalescing holes R_1, R_2 somewhat differs, in our analysis we used the average value of the radius $R = [(R_1^2 + R_2^2)/2]^{1/2}$. Within the limits of such differences in sizes, scaling behavior of coalescence does not differ. The films were placed in a Linkam LTS120 heating stage which allowed conducting optical measurements. In the experiments we employed an Olympus BX51 optical microscope equipped with an Avantes fiber spectrometer and a charge-coupled device detector with the possibility to measure the spatial distribution of the intensity of light reflected from the film. Thickness of the films and the holes was determined from the intensity of reflected nonpolarized light [21]. The experiments reported in this work were performed on films with thickness $N_f = 10$ smectic layers and holes with thickness $N_h = 8$ layers. Dynamics of coalescence was recorded with a high-speed Mikrotron EoSens video camera. The camera can continuously record a sequence of images during about two seconds to its internal memory. The start of the process of saving the images to the computer hard disk can be triggered after the beginning of coalescence. In such a way it was possible to save images recorded before, during, and after coalescence. In the measurements the operating regime of the video camera was chosen to provide a suitable frame rate, spatial resolution, and frame size at the same time. Typical recording parameters were 2500 frames per second and frame size 560×374 pixels. The used parameters enabled us to catch all essential features of coalescence at different stages of the process.

III. RESULTS AND DISCUSSION

After preparation of the sample the holes travel in the film due to diffusion and weak air flow. Occasionally they can come into contact. In such a state pairs of holes can exist for a long time (about minutes) due to the existence of attractive van der Waals forces and a potential barrier between the holes. The time of start of coalescence is rather unpredictable. Overcoming the barrier due to thermal fluctuations can take a substantial time (about minutes).

Coalescence starts from the rupture of the barrier and fast growth of the bridge between holes [Figs. 2(a) and 2(b)]. In a 3D system the driving force of coalescence of bubbles is the surface tension. In our case an edge dislocation exists between the hole and the film. The driving force for coalescence is the dislocation tension γ_d which is balanced by viscous flow outside and inside the hole. Line dislocation tension is the analog of the two-dimensional surface tension in the 3D system [17]. The tension between a thicker smectic film and thinner holes can be written in the form $\gamma_d = \Gamma b/N_f d$ [17], where b is the number of smectic layers in the Burgers vector, $b = N_f - N_h$, and Γ is the line tension of a dislocation with modulus of Burgers vector equal to the smectic layer spacing d. It is worth noting that the thickness of the holes in our experiment is not much smaller than the thickness of the surrounding film. So, coalescence dynamics is governed by the dissipation

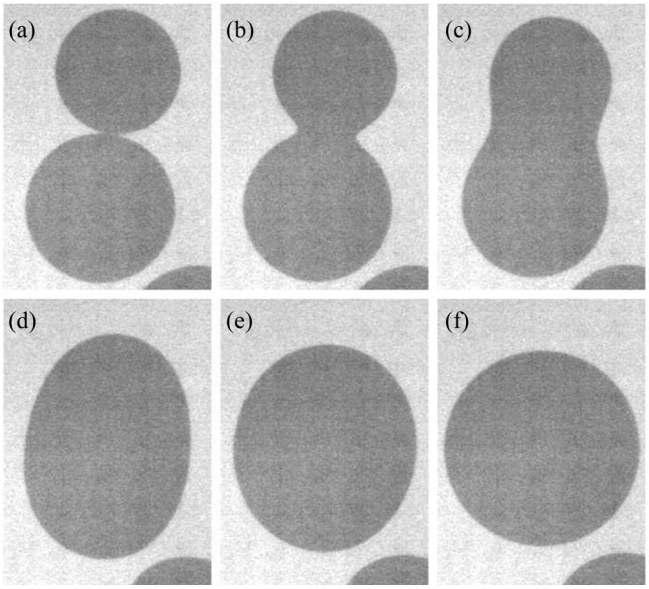

FIG. 2. Coalescence of two holes with thickness eight smectic layers in a film with thickness ten layers. Photos were taken 2.6 ms (b), 8.6 ms (c), 28.6 ms (d), 48.6 ms (e), and 198.6 ms (f) after start of coalescence. The horizontal size of the images is 159 μm.

both in the surrounding film and in the holes. Coalescence can be divided into several stages. Figure 2 shows images taken before coalescence [two circles (a)], during coalescence (b)–(e), and after coalescence [one circular domain (f)]. At the first stage the main transformations are related to the quickly growing bridge between two holes [Figs. 2(b) and 2(c)]. At the following stage the whole domain is deformed. At the final stage of coalescence we observe a slower relaxation of the domain of nearly elliptical form towards a circle that has a smaller length of the boundary with the film [Figs. 2(d)–2(f)]. The velocity of material flow at the initial stage in the region of the bridge boundary is sufficiently larger than at the final stage, when relaxation to the circular form takes place. Fast transformation of the length and form of the bridge is due to high local curvature of the bridge in the region of the contact with the film and, as a consequence, large dislocation pressure in this region. Figure 3 shows a typical temporal dependence of the bridge half length (at the initial stage) and then the smaller half size of the domain (at the later stage) for two pairs of holes with different R. The speed of coalescence decreases with increasing the size of the holes. According to optical images before the start of real coalescence a finite value H_0 of about 10 μm exists (Fig. 3). Based on optical observations we cannot state whether the holes contact in one point or along the line about $2H_0$ in length. If the circular holes contact in a point the distance between holes Δ increases as H^2/R. At $H = 10$ μm and $R = 100\,\mu$m the distance between holes $\Delta \approx 1\,\mu$m which is comparable with the resolution of our optical system. In order to minimize the influence of the finite value of H_0 on the analysis of results we further use the experimental data at $H > 1.5H_0$.

Now we analyze in detail the coalescence mechanism, test the scaling law, and determine the function $H(t)/R = F(t/\tau_R)$, where $H(t)$ is scaled by R and time t is scaled by

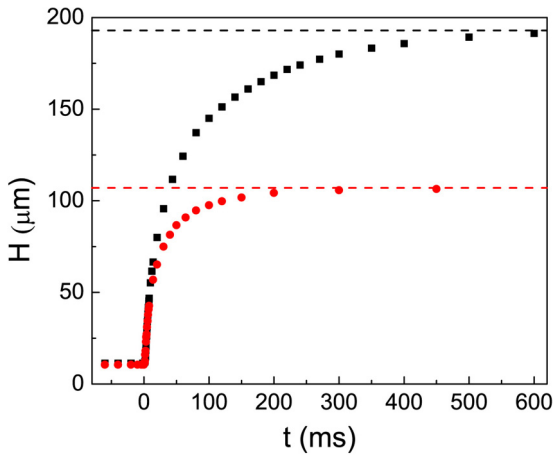

FIG. 3. The half length of the bridge $H(t)$ versus time for domains with final radius $R_f = 193\,\mu$m (■) and $R_f = 107\,\mu$m (●). Characteristic time of coalescence increases with increasing hole size.

τ_R. The times τ_R were determined by fitting the experimental data $H(t)/R$ for pairs of coalescing holes by Hopper's law and the dependence $H(t)/R = (t/\tau_R)^{1/2}$. Figure 4 shows the comparison of temporal dependence of experimental data $H(t)$ with Hopper's law (solid line) at the initial stage of coalescence. The time of coalescence start t_0 and τ_R were fitting parameters. It is clear that Hopper's law does not describe the experimental dependence well. Figure 5(a) shows the comparison of the same experimental data as in Fig. 4 with $(t/\tau_R)^{1/2}$ dependence. For such scaling the experimental data from different sets collapsed on the same curve and formed a universal dependence for $H/R < 0.7$ [points in Fig. 5(a)]. The solid curve is the dependence $H(t)/R = (t/\tau_R)^{1/2}$. In Fig. 5(b) the results are given in the log-log scale, the straight line corresponds to the power-law growth of the bridge with power 1/2. Agreement of the temporal dependence $H(t)$ with theory

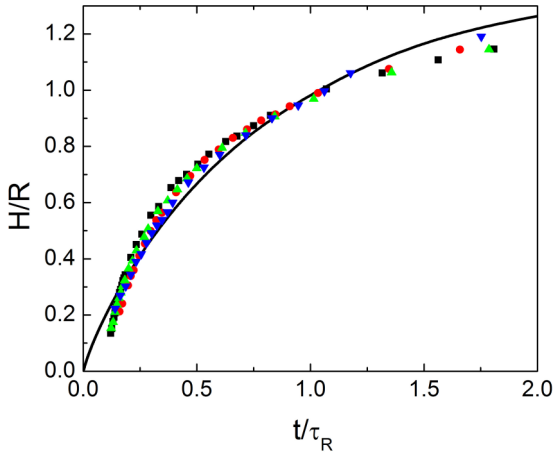

FIG. 4. Comparison of temporal dependence of the experimental data $H(t)/R$ with Hopper's law (solid curve). The radii of coalescing holes are $R_1 = 57.4\,\mu$m, $R_2 = 47.5\,\mu$m (▼); $R_1 = 77.5\,\mu$m, $R_2 = 73.5\,\mu$m (●); $R_1 = 108.7\,\mu$m, $R_2 = 98.6\,\mu$m (▲); $R_1 = 148.4\,\mu$m, $R_2 = 123.2\,\mu$m (■). Data (■, ●) correspond to the data shown in Fig. 3.

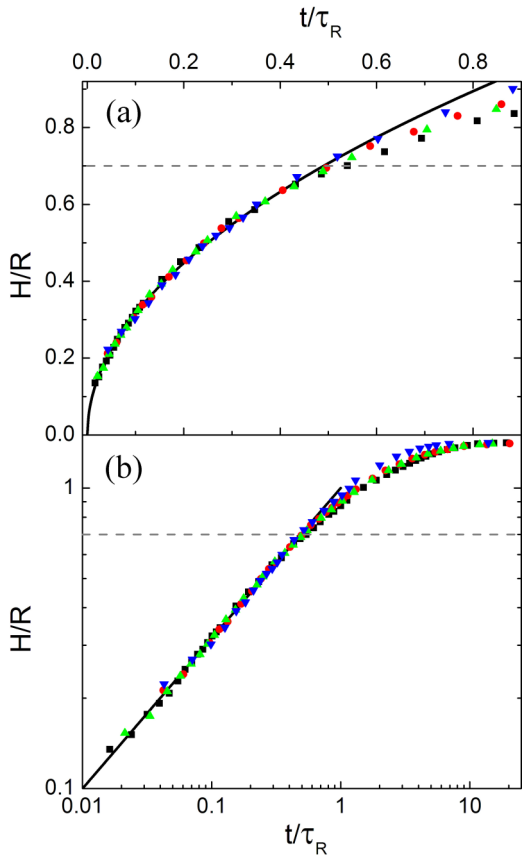

FIG. 5. (a) Experimental data on the half length of the bridge $H(t)$ scaled by the hole radius R. Time t was scaled by τ_R. The solid curve is the dependence $H(t)/R = (t/\tau_R)^{1/2}$. (b) Log-log dependence of $H(t)/R$ on t/τ_R. The solid line is the power-law dependence with exponent 1/2. Data were fitted by the dependence $H(t)/R = (t/\tau_R)^{1/2}$ in the range $H/R < 0.7$. Symbols in Fig. 5 correspond to the same experimental data as in Fig. 4.

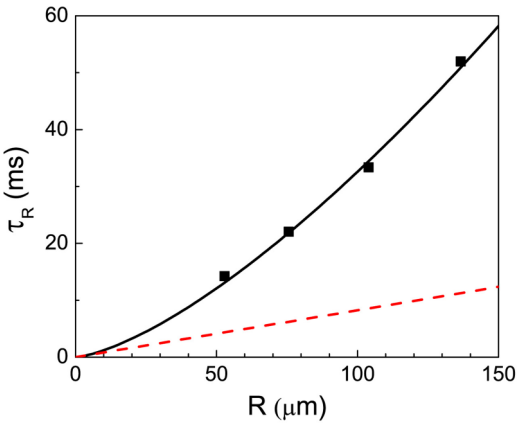

FIG. 6. Dependence of the characteristic time τ_R on R. The dashed line shows τ_R calculated from material parameters in accordance with the simple scaling $\tau_v = \eta R/\gamma$.

is quite good [Figs. 5(a) and 5(b)]. The correspondence of data from different experimental sets with the theoretical curve shows the applicability of the scaling approach for description of the temporal evolution of bridges. So, all domains coalesce in a similar way. It is worth noting that the scaling dependence is fulfilled up to large values of $H(t)/R \sim 0.7$.

The dependence of τ_R on R determined from experimental data $H(t)/R$ and the model in which temporal expansion of the bridge length is described by $H(t)/R = (t/\tau_R)^{1/2}$ is presented in Fig. 6. The increase of τ_R with R (squares) is described by the power law with power of about 1.4. Characteristic relaxation times τ_R can be compared with the theoretical time of the viscous regime $\tau_v = \eta R/\gamma$. For the 2D geometry of FSSF the surface tension γ should be replaced by $\gamma_d = \Gamma b/N_f d$. The dashed line in Fig. 6 shows the theoretical dependence $\tau(R)$ obtained using the material parameters of 8CB [29–33]. The experimentally determined τ_R are larger than theoretical values. We can explain the difference in experimentally determined and calculated τ (Fig. 6) by the influence of the viscosity of the material inside the holes [22] and by the finite viscosity of air. During coalescence the flow occurs both in the film and in the smectic material inside the holes, in air outside the film which increases the effective relaxation time. Eggers, Lister, and Stone [5] studied analytically and numerically coalescence of liquid droplets in an external fluid. In particular they found that if the viscosity of the interior and exterior fluids is equal, the speed of growth of the bridge radius decreases four times with respect to coalescence in inviscid exterior. For our case of the holes this means that the velocity of coalescence of holes of viscous material has to decrease. This correlates with our observations. Another reason for the difference in experimentally determined and calculated τ_R (Fig. 6) is the finite viscosity of air. The influence of air explains the decrease of coalescence speed during coalescence of islands [17,18]. The viscosity of air also decreases the mobility of inclusions at their diffusion in FSSFs [34,35]. It was shown [34,35] that mobility of inclusions in FSSFs depends on the coupling with the surrounding air. The Saffman length $l_S = h\eta/2\eta'$ (η and η' are the viscosity of the liquid crystal and air, and h is the film thickness) determines the contribution of the surrounding air to the reduction of mobility [34,35]. For our films Saffman length is $l_S \approx 45\ \mu$m, of the order or smaller than the size of the holes. So the surrounding air can give a contribution to the dynamics of holes.

τ_R characterize the early stage of coalescence. Using these times, the experimental data at the early stage of coalescence can be fitted on the same dependence (Fig. 5). At later times, exponential relaxation of the domain to the circular shape was found. We have to note that exponential dependence $\sim \exp(-t/\tau_e)$ was found by us directly from the experimental data $H(t)$ and for its determination there is no need to use any model. The relaxation time τ_e increases with increasing R. At present there is no theory explaining the relaxation of holes to equilibrium shape at the final stage of coalescence. We can only remind that according to Hopper's model [1–4] the relaxation of domains to the equilibrium shape has to be exponential. Such behavior was found for evolution of coalescing islands at the final relaxation stage [18].

In our analysis the dimensionless prefactor B in the dependence $H(t)/R = B(t/\tau_R)^{1/2}$ was taken to be 1. For different regimes of coalescence the prefactor B was calculated as

a function of Oh [24]. For $R \sim 10^2$ μm and our value of Oh ≈ 6 the prefactor in the viscous regime is $B_v \approx 0.8$ [24]. According to calculations [24] the prefactor B_v depends on the Ohnesorge number. However in our case decrease of Oh due to increasing R leads only to a small change of τ_R [24]. Other evaluations [22,23] also give the value of the prefactor of the order of unity. So, the assumption $B_v = 1$ used in our analysis is reasonable.

In summary, we performed experiments of coalescence of holes in free-standing films. Coalescence of holes can be regarded as a two-dimensional analog of 3D coalescence of bubbles in liquid. Comparison of the experimental data on the temporal transformation of bridges with the existing theory have shown that (i) scaling laws are applicable for the description of the peculiarities of coalescence of holes, and (ii) the initial stage of coalescence occurs with a power-law dependence of the bridge length $H(t)/R \sim (t/\tau_R)^{1/2}$. Relaxation of domains to the equilibrium shape is exponential.

ACKNOWLEDGMENT

The reported study was supported by the Russian Science Foundation under Grant No. 18-12-00108.

[1] R.W. Hopper, J. Am. Ceram. Soc. (Commun.) **67**, C-262 (1984).
[2] R. W. Hopper, J. Fluid Mech. **213**, 349 (1990).
[3] R. W. Hopper, J. Fluid Mech. **243**, 171 (1992).
[4] R. W. Hopper, J. Am. Ceram. Soc. **76**, 2947 (1993).
[5] J. Eggers, J. R. Lister, and H. A. Stone, J. Fluid Mech. **401**, 293 (1999).
[6] M. Wu, T. Cubaud, and C. Ho, Phys. Fluids **16**, L51 (2004).
[7] D. G. A. L. Aarts, H. N. W. Lekkerkerker, H. Guo, G. H. Wegdam, and D. Bonn, Phys. Rev. Lett. **95**, 164503 (2005).
[8] W. Yao, H. J. Maris, P. Pennington, and G. M. Seidel, Phys. Rev. E **71**, 016309 (2005).
[9] U. Delabre and A-M. Cazabat, Phys. Rev. Lett. **104**, 227801 (2010).
[10] J. D. Paulsen, J. C. Burton, and S. R. Nagel, Phys. Rev. Lett. **106**, 114501 (2011).
[11] J. D. Paulsen, J. C. Burton, S. R. Nagel, S. Apparthural, M. T. Harris, and O. A. Basaran, Proc. Natl. Acad. Sci. USA **109**, 6857 (2012).
[12] J. D. Paulsen, Phys. Rev. E **88**, 063010 (2013).
[13] X. Xia, C. He, and P. Zhang, Proc. Natl. Acad. Sci. USA **116**, 23467 (2019).
[14] Q. Zhang, X. Jiang, D. Brunello, T. Fu, C. Zhu, Y. Ma, and H. Z. Li, Phys. Rev. E **100**, 033112 (2019).
[15] B. M. Shipilevsky, Phys. Rev. E **100**, 062121 (2019).
[16] D. H. Nguyen, Ph.D. dissertation, University of Colorado, Boulder, 2011, https://scholar.colorado.edu/phys_gradetds/41.
[17] R. Stannarius and K. Harth, in *Liquid Crystals with Nano and Microparticles*, edited by J. P. F. Lagerwal and G. Scalia (World Scientific, Singapore, 2017); pp. 401–405, and references therein.
[18] N. S. Shuravin, P. V. Dolganov, and V. K. Dolganov, Phys. Rev. E **99**, 062702 (2019).
[19] P. V. Dolganov, N. S. Shuravin, E. I. Kats, and V. K. Dolganov, JETP Lett. **110**, 545 (2019).
[20] Z. Qi, Ph.D. dissertation, University of Colorado, 2015, https://scholar.colorado.edu/phys_gradetds/172.
[21] P. Pieranski, L. Beliard, J.-Ph. Tourellec, X. Leoncini, C. Furtlehner, H. Dumoulin, E. Riou, B. Jouvin, J. P. Fénerol, Ph. Palaric, J. Hueving, B. Cartier, and I. Kraus, Physica A **194**, 364 (1993).
[22] J. D. Paulsen, R. Carmigniani, A. Kannan, J. C. Burton, and S. R. Nagel, Nat. Commun. **5**, 3182 (2014).
[23] J. P. Munro, C. R. Antony, O. A. Basaran, and J. R. Lister, J. Fluid Mech. **773**, R3-1 (2015).
[24] C. R. Anthony, P. M. Kamat, S. S. Thete, J. P. Munro, J. R. Lister, M. T. Harris, and O. A. Basaran, Phys. Rev. Fluids **2**, 083601 (2017).
[25] K. Harth and R. Stannarius, Ferroelectrics **468**, 92 (2014).
[26] P. V. Dolganov, E. I. Kats, and V. K. Dolganov, JETP Lett. **106**, 229 (2017).
[27] P. V. Dolganov, J. Mol. Liq. **267**, 249 (2018).
[28] P. V. Dolganov, P. Cluzeau, and V. K. Dolganov, Liq. Cryst. Rev. **7**, 1 (2019).
[29] A. Zywocinski, F. Picano, P. Oswald, and J. Ch. Gèminard, Phys. Rev. E **62**, 8133 (2000).
[30] P. Oswald, F. Picano, and F. Caillier, Phys. Rev. E **68**, 061701 (2003).
[31] D. Davidov, C. R. Safinya, M. Kaplan, S. S. Dana, R. Schaetzing, R. J. Birgeneau, and J. D. Litster, Phys. Rev. B **19**, 1657 (1979).
[32] D. A. Dunmur and W. H. Miller, J. Phys. Colloq. **40(C3)**, C3-141 (1979).
[33] F. Schneider, Phys. Rev. E **74**, 021709 (2006).
[34] Z. H. Nguyen, M. Atkinson, C. S. Park, J. Maclennan, M. Glaser, and N. Clark, Phys. Rev. Lett. **105**, 268304 (2010).
[35] A. Eremin, S. Baumgarten, K. Harth, R. Stannarius, Z. H. Nguyen, A. Goldfain, C. S. Park, J. E. Maclennan, M. A. Glaser, and N. A. Clark, Phys. Rev. Lett. **107**, 268301 (2011).